KNH2-KH: A metal amide-hydride solid solution

UNIVERSITÀ DEGLI STUDI DI TORINO

KNH_2 - KH: a metal amide - hydride solid solution

Antonio Santoru*[a, b], Claudio Pistidda[a], Magnus H. Sørby[c], Michele R. Chierotti[b], Sebastiano Garroni[d], Eugenio Pinatel[b], Fahim Karimi[a], Hujun Cao[a], Nils Bergemann[a], Thi T. Le[a], Julián Puszkiel[a, e], Roberto Gobetto[b], Marcello Baricco[b], Bjørn C. Hauback[c], Thomas Klassen[a] and Martin Dornheim[a]

We report for the first time the formation of a metal amide-hydride solid solution. The dissolution of KH into KNH_2 leads to an anionic substitution, which decreases the interaction among NH_2^- ions. The rotational properties of the high temperature polymorphs of KNH_2 are thereby retained down to room temperature.

The amides of alkaline and alkaline-earth metals were discovered and independently investigated by J. L. Gay-Lussac and H. Davy in the early 19th century[1, 2]. Further studies on their properties were performed towards the end of the same century, most systematically from A. W. Titherley[3]. The determination of their crystal structures was possible only after the 1930s with the studies of Juza et al.,[4-10] later continued by Jacobs et al.[11, 12]

At that time this class of compounds was mostly used for organic synthesis. However, more recently, metal amides – metal hydrides mixtures have been proven to be suitable for reversible hydrogen storage.[13] Furthermore, metal amides – metal borohydrides systems are regarded as potential solid state ionic conductors.[14]

The structural and thermal properties of light-weight amides prepared by reaction of metal hydrides with ammonia have been systematically examined by *in situ* diffraction experiments.[15] While the reaction mechanism and products reported in previous studies were confirmed for the amides of lithium and sodium,[16-18] the formation of new K-N-H based intermediates was suggested for potassium amide. The same intermediates were proven to play a role in the desorption reactions of the K-Mg-N-H system.[19] These intermediates are isolated here in the KNH_2-KH system and, to the best of our knowledge, identified as the first metal amide-hydride solid solution.

The crystal structures of pristine potassium amide and potassium hydride have already been investigated by X-ray and neutron diffraction.[7, 8, 12, 20-22] Potassium hydride is known to crystallize in a cubic rock-salt type structure with space group (s.g.) $Fm\bar{3}m$ and no polymorph changes are expected in the temperature range from room temperature (RT) to 390 °C.[21] For potassium amide, the stable polymorph at RT is monoclinic with s.g. $P2_1/m$.[7] Upon heating this phase transforms into a tetragonal structure with in $P4/nmm$ at 54 °C.[12] The latter phase is stable only in a narrow temperature range; and already above 75 °C the stability of a cubic phase ($Fm\bar{3}m$) prevails.[12, 20, 22] An increase of symmetry is therefore reached with the two phase transitions at higher temperature. The explanation of the symmetry changes resides in the increasingly high orientational disorder of the amide anions, as proven by powder neutron diffraction (PND), quasielastic incoherent neutron scattering and orientation-dependent deuterium spin lattice relaxation.[20, 23, 24] If the maximum temperature upon heating is kept below the decomposition temperature of KNH_2 (ca. 340 °C), the two phase transitions and the associated rotational dynamics should be reversible on cooling.

This is in agreement with the present *in situ* synchrotron radiation powder X-ray diffraction experiment (SR-PXD) on KNH_2 (ESI). When a 0.5 KNH_2 + 0.5 KH mixture was investigated, the expected phase transformations of KNH_2 took place, but the interaction of KNH_2 and KH in the temperature range between 100 °C and 270 °C led to the formation of a new cubic structure (Figure 1 a).†

PND at 270 °C of a potassium deuteramide - potassium deuteride mixture confirmed the presence of a single cubic phase at this temperature (Figure 1 b).‡

[a] *Nanotechnology Department, Helmholtz-Zentrum Geesthacht Max-Planck Straße 1, 21502, Geesthacht, Germany*
[b] *Department of Chemistry and NIS centre, University of Torino, V. Giuria 7, 10125, Torino, Italy*
[c] *Physics Department, Institute for Energy Technology (IFE), P.O. Box 40, NO-2027 Kjeller, Norway*
[d] *Department of Chemistry and Pharmacy, University of Sassari, V. Vienna 2, 07100, Sassari, Italy*
[e] *Department of Physicochemistry of Materials,Consejo Nacional de Investigaciones Científicas y Técnicas (CONICET) y Centro Atómico Bariloche, Av. Bustillo km 9500, San Carlos de Bariloche, CP 8400, Argentina*

Electronic Supplementary Information (ESI) available: powder X-ray and neutron diffractograms, Rietveld refinements, thermal decomposition, experimental details. See DOI: 10.1039/x0xx00000x

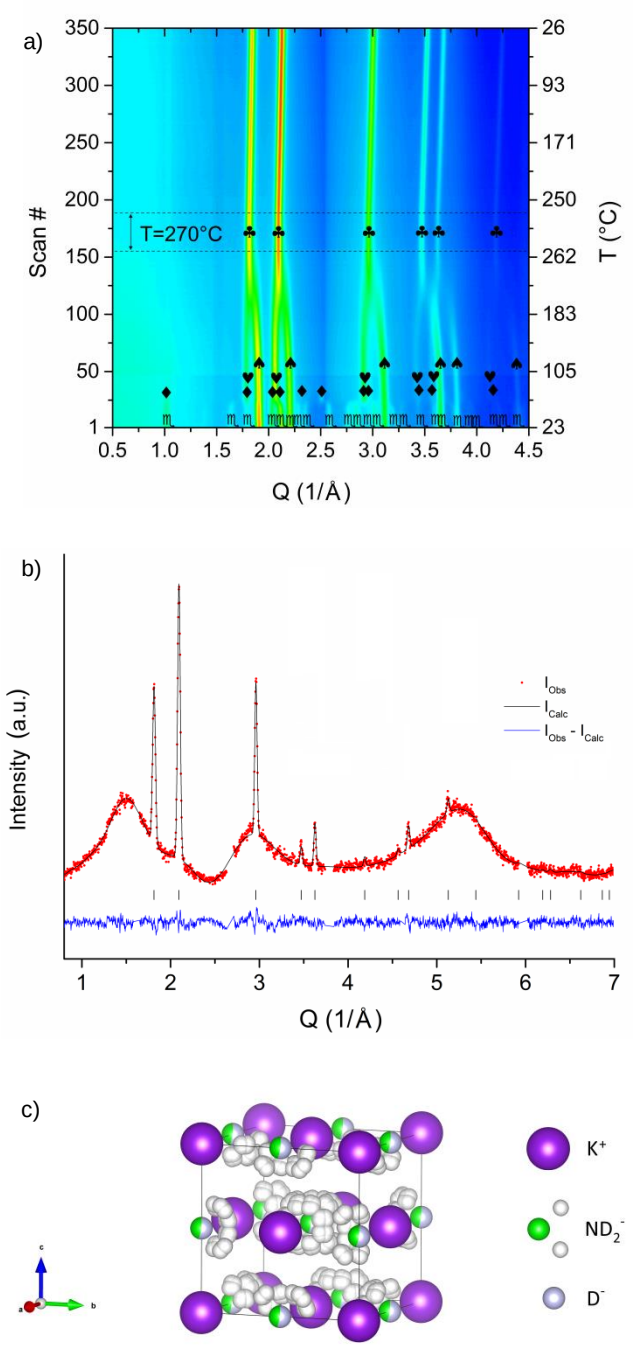

Figure 1. a) *In situ* SR-PXD experiment on the 0.5 KNH_2 + 0.5 KH sample. ♏ = KNH_2 (P21/*m*), ♦ = KNH_2 (P4/*nmm*), ♥ = KNH_2 (F*m*$\bar{3}$*m*), ♠ = KH (F*m*$\bar{3}$*m*), ♣ = new phase (F*m*$\bar{3}$*m*). b) PND pattern of the nominal 0.5 KND_2 + 0.5 KD mixture annealed up to 270 °C and kept in isothermal condition during the data collection. Rwp(%) = 2.8 (corrected for background). The wavy background was originated from the quartz sample holder (see Supporting Information). c) Structural model of the cubic phase (s.g. F*m*$\bar{3}$m) of composition $K(ND_2)_{0.46}D_{0.54}$ obtained after the Rietveld refinement, taking into account the anionic substitution at the position (0.5 0.5 0.5) and the orientational disorder of amide anions.

The structure was solved assuming an ionic crystal with unaltered positions for the potassium cations and partially occupied sites at the original positions of amide and hydride anions. Indeed the formation of a solid solution is highly favorable due to the structural similarities between the two cubic polymorphs of KNH_2 and KH (same space group, same cation, same charge for the anions, similar lattice constants).

The local symmetry of the deuteramide groups is compatible with the s.g. *Fm*$\bar{3}$*m* only assuming rotational dynamics and orientational disorder. In this case the restrictions imposed from both the s.g. and rigid amide groups resulted in partially occupied sites (multiplicity = 192) for the deuterium atoms of each amide group (Figure 1 c).

The final Rietveld refinement[25, 26] of the PND pattern (Figure 1 b) confirmed the structural model, i.e. the formation of a potassium amide-hydride solid solution. To the best of our knowledge, no similar cases have been reported so far for other alkaline metal amides-metal hydrides mixtures.

The similarity of chemical environment between the starting materials and the x KNH_2 + (1- x) KH samples at different compositions (x = 0.1, 0.5, 0.9) after annealing was verified by ^{1}H magic angle spinning solid-state NMR (MAS SSNMR), see Figure 2.§

No significant shifts are observed while the integral values perfectly reflect the composition of the solid solution. Furthermore, the same T_1 ^{1}H value (46 s) for both signals supports the formation of a solid solution since it indicates that spin diffusion is active. This is only possible if they belong to the same phase or in the case of homogeneous samples on a nanometer scale.[27] Direct evidence of the solid solution formation is provided by the ^{1}H double-quantum (DQ) MAS SSNMR experiment (Figure 2 b). Indeed, the observed DQ correlation between the KNH_2 (-3.2 ppm) and KH (4.8 ppm) signals implies that they are in close spatial proximity each other (less than 5 Å). This is only possible if they are intimately related as in a solid solution.[28, 29] Similar correlation, although much weaker, is observed for the sample before annealing (Supporting Information), which can be explained with the formation of a small fraction of solid solution due to the fast rotation and slightly increased temperature during the NMR experiment.

The effect of the starting composition of the mixtures on the final structure was studied by means of *in situ* SR-PXD. A linear relationship was found between the unit cell parameter of the cubic phase at T = 270 °C and the molar fraction of amide anions (Figure 3 and Table 1) as expected from Vegard's law.[30] This indicates volumes of mixing close to zero and, therefore, an almost ideal behavior for the solid solution ($\Delta H_{mix} \approx 0$).

It is noteworthy that, for the compositions x = 0.1, 0.3, 0.5, 0.7, the structure did not change during the cooling process down to RT, except for the thermal contraction of the unit cell volume (more details in Table 1 and in Supporting Information).

It appears that the addition of potassium hydride can stabilize the cubic geometry, which retains the rotation of the amide anions even at RT. A similar behavior was previously reported for the sodium borohydride - sodium chloride systems, at different temperature (T = - 81 °C).[31] *Ex situ* PXD of annealed samples (x = 0.3, 0.5, 0.7, 0.9) collected with a Bragg Brentano diffractometer proves the coexistence of at least two different cubic structures. The composition x = 0.1, however, presented unchanged cubic phase (see Supporting Information). At the

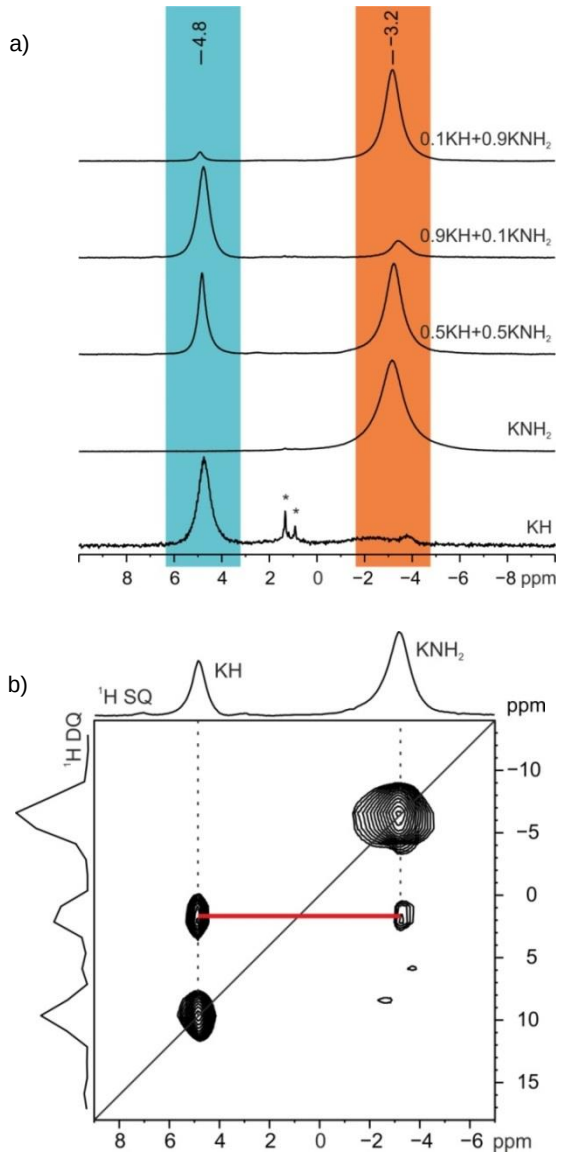

Figure 2. a) ^{1}H (400.23 MHz) MAS SSNMR spectra of starting reagents and x KNH_2 + (1 - x) KH samples at different composition (x = 0.1, 0.5, 0.9) after annealing recorded with a spinning speed of 32 kHz. Asterisks denote impurities. b) 2D ^{1}H (400.23 MHz) DQ MAS SSNMR spectrum of the KNH_2 + KH (x = 0.5) after annealing recorded with a spinning speed of 32 kHz. The red line highlights the DQ correlation between the KH and KNH_2 signal.

composition x = 0.9, coexistence of the cubic and monoclinic phases was found. These results suggest the presence of a two phase field at RT. Nevertheless, even in the cases where phase segregation occurred, both cubic structures were proven to be unchanged even after several months, hence a complete transformation back to the pure monoclinic phase of KNH_2 and cubic phase of KH did not occur.

Noteworthy, the same structures are formed simply by mechanochemical treatments of the starting reactants. In some cases (x = 0.1, 0.3 and 0.9) manual grinding is enough to promote the formation of detectable amounts of $K(NH_2)_xH_{(1-x)}$ solid solution. These species are therefore easily formed and are expected to be possibly identified as reaction products or intermediates in future studies of amide-based systems containing potassium.

Table 1. Structural details of the $K(NH_2)_xH_{(1-x)}$ phase at different compositions

x [a]	x [b]	*a* / Å [c]	α / K^{-1} [d]	*a* / Å [e]
0	0	5.74934(14)	3.19(2)E-05	5.70390(14)
0.1	0.070(5)	5,81372(13)	5.30(1)E-05	5.73769(13)
0.3	0.240(8)	5,8989(2)	5.88(2)E-05	5.8134(2)
0.5	0.490(14)	6.0003 (2)	6.32(1)E-05	5.9060(2)
0.7	0.72(3)	6,07768(12)	6.83(1)E-05	5.98320(12)
0.9	0.91(3)	6,14553(14)	6.83(2)E-05	6.04230(14)
1	1	6,17667(8)	7.38(1)E-05	6.06473 (8)

[a] Nominal composition and [b] Refined composition (molar fraction) of KNH_2 [c] Refined cell parameters at 270 °C [d] Calculated linear thermal expansion coefficients [e] Calculated cell parameters at 20 °C. Estimated standard deviations are given in parentheses.

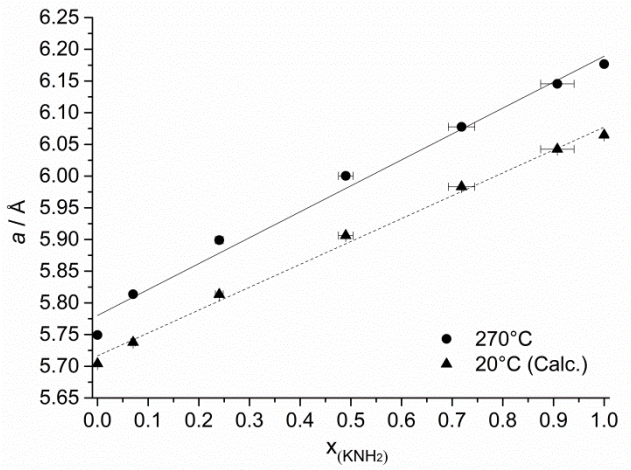

Figure 3. Unit cell parameters (dots) obtained by *in situ* SR-PXD experiments in isothermal conditions (T = 270 °C) as a function of the potassium amide content and corresponding linear fit (continuous line). The values for T = 20 °C (triangles) were calculated using the thermal expansion coefficient of each phase and then fitted (dotted line). The error bars for molar fractions and cell parameters were calculated considering the errors of the Rietveld process.

To the best of our knowledge, amide/hydride solid solutions were not reported so far. In this sense, the chemistry of the K-based amide/hydride system is interestingly peculiar and differs substantially from the one of the other alkaline metal amides/hydrides.

The research leading to these results has received funding from the European Marie Curie Actions under ECOSTORE grant agreement no. 607040. The help of the beamline scientists Francisco Martinez Casado, Dorthe Haase, Olivier Balmes, (MAX-lab – Lund, Sweden), Martin Etter and Jozef Bednarcik (DESY – Hamburg, Germany) is thankfully acknowledged. A.S. thanks the research groups of Turin University, Sassari University and IFE for the fruitful discussion and Dr. Klaus Taube, coordinator of the ECOSTORE project, for providing the essential networking opportunities.

Notes and references

† The in situ SR-PXD experiments were performed at the diffraction beamline I711, MAX Lab (Lund, Sweden) and at the diffraction beamline P02, DESY (Hamburg,

Germany) (monochromatic beams of $\lambda \approx 0.99$ Å and ≈ 0.2 Å were employed respectively). The in situ cells and the procedure used are described elsewhere.[19, 32]
‡ PND was performed at the PUS instrument at the JEEP II reactor at IFE, Norway.[33] Neutrons with $\lambda = 1.5539$ Å were provided by a focussing Ge(511) monochromator at 90° take-off angle. Data was collected in the range $2\theta = 10\text{-}130°$ ($\Delta 2\theta = 0.05°$) by 2 detector banks each with 7 vertically stacked position sensitive detectors. The sample was contained in an argon-filled quartz tube with 6 mm diameter placed inside an in-house built furnace. The structure solution was carried out using the software "FOX"[34]. The Rietveld refinement was performed by means of the software GSAS[35] and the EXPGUI graphic interface[36].
§ Solid-state NMR experiments were run on a Bruker AVANCE II 400 instrument operating at 400.23 MHz for ^{1}H and equipped with a 2.5 mm probe. The ^{1}H MAS spectra were acquired at the spinning speed of 32 kHz with the DEPTH sequence ($\pi/2 - \pi - \pi$) for the suppression of the probe background signal (^{1}H 90° = 2.5 µs; scans = 16; relaxation delay = 53 s). 2D ^{1}H DQ MAS experiments were performed at 32 kHz with the back-to-back (BABA) recoupling pulse sequence with excitation times of one rotor period (^{1}H 90°= 2.5 µs; 32 scans; t_1 increments = 46; relaxation delay = 53 s). ^{1}H scale was calibrated with adamantane (^{1}H signal at 1.87 ppm) as external standards.

1. J. L. Gay and L. J. Thenard, *Journal*, 1809, **32**, 23-39.
2. H. Davy, *Philosophical Transactions of the Royal Society of London*, 1808, **98**, 333-370.
3. A. W. Titherley, *Journal of the Chemical Society, Transactions*, 1894, **65**, 504-522.
4. R. Juza, *Angewandte Chemie*, 1964, **76**, 290-300.
5. R. Juza, *Zeitschrift für anorganische und allgemeine Chemie*, 1937, **231**, 121-135.
6. R. Juza, K. Fasold and C. Haeberle, *Zeitschrift für anorganische und allgemeine Chemie*, 1937, **234**, 75-85.
7. R. Juza, H. Jacobs and W. Klose, *Zeitschrift für anorganische und allgemeine Chemie*, 1965, **338**, 171-178.
8. R. Juza and H. Liedtke, *Zeitschrift für anorganische und allgemeine Chemie*, 1957, **290**, 205-208.
9. R. Juza and K. Opp, *Zeitschrift für anorganische und allgemeine Chemie*, 1951, **266**, 313-324.
10. R. Juza, H. H. Weber and K. Opp, *Zeitschrift für anorganische und allgemeine Chemie*, 1956, **284**, 73-82.
11. H. Jacobs, *Zeitschrift für anorganische und allgemeine Chemie*, 1971, **382**, 97-109.
12. H. Jacobs and E. Von Osten, *Zeitschrift für Naturforschung*, 1976, **31**, 385-386.
13. P. Chen, Z. Xiong, J. Luo, J. Lin and K. L. Tan, *Nature*, 2002, **420**, 302-304.
14. M. Matsuo, A. Remhof, P. Martelli, R. Caputo, M. Ernst, Y. Miura, T. Sato, H. Oguchi, H. Maekawa, H. Takamura, A. Borgschulte, A. Züttel and S.-i. Orimo, *Journal of the American Chemical Society*, 2009, **131**, 16389-16391.
15. C. Pistidda, A. Santoru, S. Garroni, N. Bergemann, A. Rzeszutek, C. Horstmann, D. Thomas, T. Klassen and M. Dornheim, *The Journal of Physical Chemistry C*, 2015, **119**, 934-943.
16. W. I. F. David, M. O. Jones, D. H. Gregory, C. M. Jewell, S. R. Johnson, A. Walton and P. P. Edwards, *Journal of the American Chemical Society*, 2007, **129**, 1594-1601.
17. J. W. Makepeace, M. O. Jones, S. K. Callear, P. P. Edwards and W. I. F. David, *Physical Chemistry Chemical Physics*, 2014, **16**, 4061-4070.
18. H. Yamamoto, H. Miyaoka, S. Hino, H. Nakanishi, T. Ichikawa and Y. Kojima, *International Journal of Hydrogen Energy*, 2009, **34**, 9760-9764.
19. A. Santoru, S. Garroni, C. Pistidda, C. Milanese, A. Girella, A. Marini, E. Masolo, A. Valentoni, N. Bergemann, T. T. Le, H. Cao, D. Haase, O. Balmes, K. Taube, G. Mulas, S. Enzo, T. Klassen and M. Dornheim, *Physical Chemistry Chemical Physics*, 2016, **18**, 3910-3920.
20. M. Müller, J. Senker, B. Asmussen, W. Press, H. Jacobs, W. Kockelmann, H. M. Mayer and R. M. Ibberson, *The Journal of chemical physics*, 1997, **107**, 2363-2373.
21. V. G. Kuznetsov and M. M. Shkrabkina, *J Struct Chem*, **3**, 532-537.
22. M. Müller, B. Asmussen, W. Press, J. Senker, H. Jacobs, H. Büttner, W. Kockelmann and R. M. Ibberson, *Physica B: Condensed Matter*, 1997, **234–236**, 45-47.
23. M. Müller, B. Asmussen, W. Press, J. Senker, H. Jacobs, H. Büttner and H. Schober, *The Journal of chemical physics*, 1998, **109**, 3559-3567.
24. J. Senker, *Solid State Nuclear Magnetic Resonance*, 2004, **26**, 22-35.
25. H. M. Rietveld, *Journal*, 1967, **22**, 151-152.
26. H. M. Rietveld, *Journal*, 1969, **2**, 65-71.
27. K. Gaglioti, M. R. Chierotti, F. Grifasi, R. Gobetto, U. J. Griesser, D. Hasa and D. Voinovich, *CrystEngComm*, 2014, **16**, 8252-8262.
28. D. Braga, L. Chelazzi, F. Grepioni, E. Dichiarante, M. R. Chierotti and R. Gobetto, *Crystal Growth & Design*, 2013, **13**, 2564-2572.
29. M. R. Chierotti and R. Gobetto, *CrystEngComm*, 2013, **15**, 8599-8612.
30. L. Vegard, *Zeitschrift für Physik*, **5**, 17-26.
31. J. E. Olsen, P. Karen, M. H. Sørby and B. C. Hauback, *Journal of Alloys and Compounds*, 2014, **587**, 374-379.
32. U. Bösenberg, C. Pistidda, M. Tolkiehn, N. Busch, I. Saldan, K. Suarez-Alcantara, A. Arendarska, T. Klassen and M. Dornheim, *International Journal of Hydrogen Energy*, 2014, **39**, 9899-9903.
33. B. C. Hauback, H. FjellvåG, O. Steinsvoll, K. Johansson, O. T. Buset and J. Jørgensen, *Journal of Neutron Research*, **8**, 215-232.
34. V. Favre-Nicolin and R. Cerny, *Journal of Applied Crystallography*, 2002, **35**, 734-743.
35. A. C. L. a. R. B. V. Dreele, *Los Alamos National Laboratory Report LAUR 86-748*, 2000.
36. B. Toby, *Journal of Applied Crystallography*, 2001, **34**, 210-213.

KNH_2 - KH: a metal amide - hydride solid solution

Antonio Santoru*, Claudio Pistidda, Magnus H. Sørby, Michele R. Chierotti, Sebastiano Garroni, Eugenio Pinatel, Fahim Karimi, Hujun Cao, Paolo C. Vioglio, Nils Bergemann, Thi T. Le, Julián Puszkiel, Roberto Gobetto, Marcello Baricco, Bjørn C. Hauback, Thomas Klassen and Martin Dornheim

Experimental details.

Synthesis. KH (30 wt% dispersion in mineral oil) was purchased from Sigma-Aldrich. Before usage the oil was removed by washing 3 times with hexane in vacuum filtration. KNH_2 was synthesized by reactive ball milling of the dry potassium hydride powder in a Fritsch Pulverisette 6, at 400 RPM, with a BPR ca. 20:1, under 7 bar of ammonia atmosphere. The reaction vessel (a high pressure vial from Evicomagnetics) was evacuated and refilled with ammonia 4 times, for a total milling time of 18 h. Both the starting materials (KH and KNH_2) were then independently ball milled in a SPEX 8000 mill for 600 minutes to obtain a finer powder. The mixtures of KNH_2 and KH were prepared grinding the two reactants for 5 minutes in an agate mortar. The annealed samples were prepared in a thermal reactor from Parr Instruments, heating at 270 °C under Argon atmosphere for 1 h.
The ball milled samples were prepared using a SPEX 8000 Mill, milling the powder for 5h with a BPR of 10:1. Hardened steel vials and balls were used.
Potassium deuteramide (KND_2) was synthesized by thermal treatment of metallic potassium under 5 bar of deuterated ammonia (ND_3) for 16 h at 300 °C in an autoclave from Parr Instruments. The reaction can be written as: $K + ND_3 \rightarrow KND_2 + 1 / 2\ D_2$
Potassium deuteride was synthesize ball milling pure potassium under 50 bar of deuterium (D_2) for 36 h with a rotational speed of 600 rpm and a ball to powder ratio of 60:1. Potassium (98 % purity) under mineral oil was purchased as commercial product from Sigma Aldrich. A cube of 1.1 g approximately was cut. Before use, the oil was removed washing with hexane. In addition the material surface was polished with a sharp blade.
The diffractograms on the ball milled samples (Figure S2) were collected with a Bruker D8 Advance diffractometer in Bragg-Brentano geometry using a General Area detector and a Cu X-ray source. The sample was investigated using an airtight sample holder from Bruker. The incoherent scattering of the Poly (methyl methacrylate) dome is responsible for the bump observed between 1 and 2 $Å^{-1}$ in all the diffractograms (Figure S2).
The diffractograms on the annealed samples (Figure S3) were performed in the 2θ range 2° – 90° (step size of 0.017°, time per step 200 s) using a laboratory diffractometer (Panalytical X'Pert Pro Multipurpose Diffractometer) equipped with Ni filtered Cu source in Debye-Scherrer geometry. Samples were sealed into boron silica glass capillaries of internal diameter 0.8 mm in a protected atmosphere.
The sample handling was performed in an Argon circulation glove box, with oxygen and moisture concentrations lower than 2 ppm.
The scattering images obtained by *in situ* synchrotron X-ray diffraction were integrated with the program Fit2D.[1] Rietveld refinement was performed by means of MAUD program (Material Analysis Using Diffraction)[2] on the diffractograms selected for phase identification and determination of the cell parameters (Figures S5, S6, S7, S8, S9). In any case structural models from the literature were used for the known phases of KNH_2 and KH. For the new $K(NH_2)_xH_{(1-x)}$ phases a general structural model was obtained using FOX software[3] on the pattern obtained by *in situ* powder neutron diffraction on the sample with nominal composition x = 0.5 and then adapted for the other different compositions. The occupancies for the amide and hydride anions were calculated and fixed in order to be in agreement with the refined composition of the room temperature pattern. The Rietveld refinement of the neutron diffraction pattern was performed with GSAS software.[4]

Linear expansion coefficients and related structural properties.

The linear thermal expansion coefficients reported in Table 1 were calculated according to the following formula:
$\alpha_L = (a_2 - a_1) / [a_1 (T_2 - T_1)]$, where $T_2 > T_1$ and $a_2 > a_1$.
The cell parameters "a_1" and the temperatures "T_1" are referred to the diffractograms collected during the cooling process, since in that interval only one $K(NH_2)_xH_{(1-x)}$ was present. T_2 = 270 °C for all the samples. For the compositions x = 0, 0.1, 0.3, 0.5, 0.7 the calculations are referred to $T_1 \approx$ RT while for the compositions x = 0.9 and x = 1, the diffractograms corresponding to T_1 = 48 °C and T_1 = 82 °C were selected respectively, due to the phase transformations occurring at lower temperatures.

The obtained linear expansion coefficient was then used to calculate the cell parameter expected at T_1 = 20 °C for the cubic polymorph of each composition (also reported in Table 1). Even though for the pure KNH_2 the cubic polymorph does not exist at room temperature (in normal pressure conditions), the cell parameter calculated with the linear expansion coefficient of the cubic form of KNH_2 is in good agreement with the values expected by the linear behavior (Figure 4 – Main article). The explanation most probably resides in the structural similarities between the different polymorphs of KNH_2. Indeed, considering the cubic structure highlighted in Figure S1, an element of pseudo-cubic symmetry with comparable interatomic distances can be easily identified also in the monoclinic and tetragonal polymorphs.

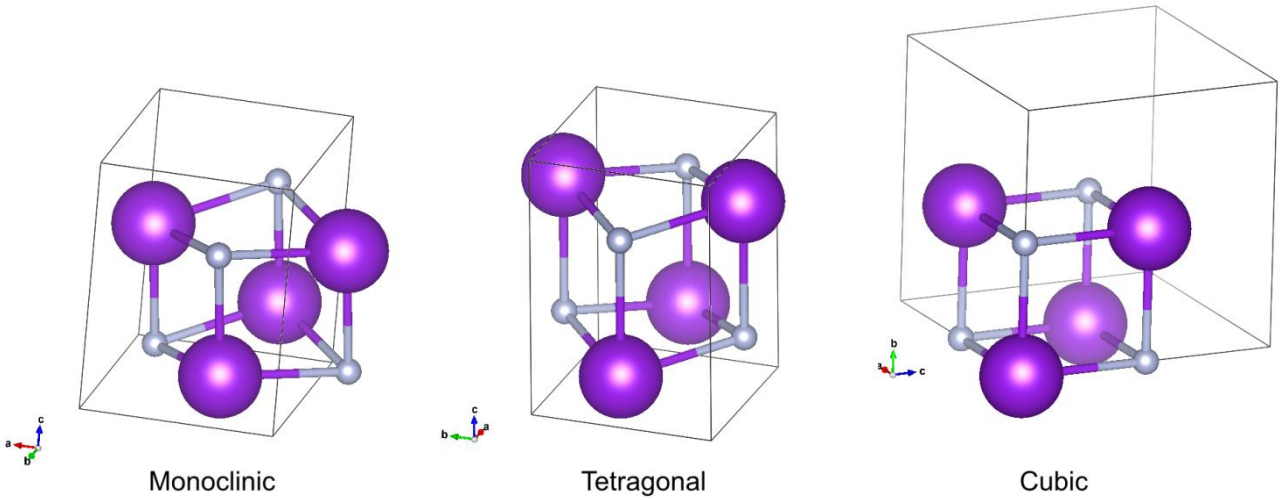

Figure S1. Structural similarities between the different polymorphs of KNH_2. The hydrogen atoms of the NH_2 groups were omitted for clarity.

Effect of ball milling

The interaction between KNH_2 and KH under mechanochemical or thermal input was studied for different compositions. The mechanical energy transfer induces a chemical reaction of the compounds already after 5 h. *Ex situ* PXD on the ball milled samples (Figure S2) shows a complete disappearance of the monoclinic polymorph of potassium amide. For all the compositions two different cubic structures coexist, namely an “amide rich” and a “hydride rich” structure. Noteworthy, the formation of a monoclinic polymorph is not observed even after several months.

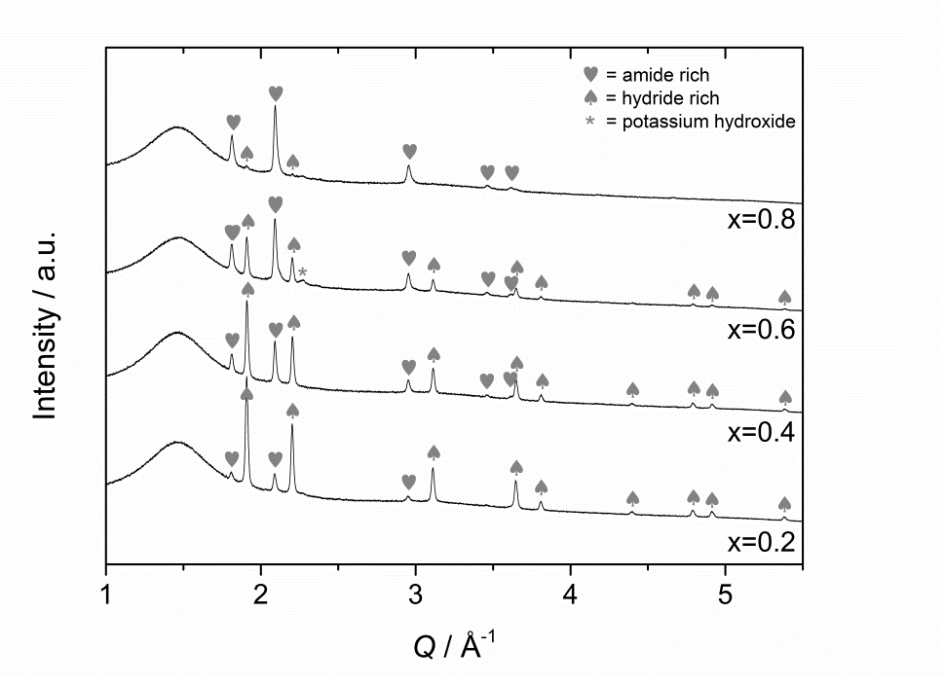

Figure S2. Diffractograms on the x KNH_2 + (1-x) KH samples collected after mechanochemical treatment.

Effect of annealing

The compositions 0.1, 0.3, 0.5, 0.7, 0.9 were studied promoting the reaction by thermal treatment up to 270 °C. *Ex situ* PXD on the annealed samples (Figure S3) confirmed that, also by thermal input, KNH_2 and KH mutually reacted to form at least two cubic phases (compositions x = 0.3, 0.5, 0.7) and only close to the lower extreme of the compositional range (x = 0.1) one single cubic phase was found, probably stabilized by the high relative amount of potassium hydride. For the composition x = 0.9, coexistence of the cubic and monoclinic phase was found. Due to the fact that amide anions can be hosted in a single cubic lattice only for certain compositions (approximately x = 0.1), these results suggest a two phase field at room temperature.

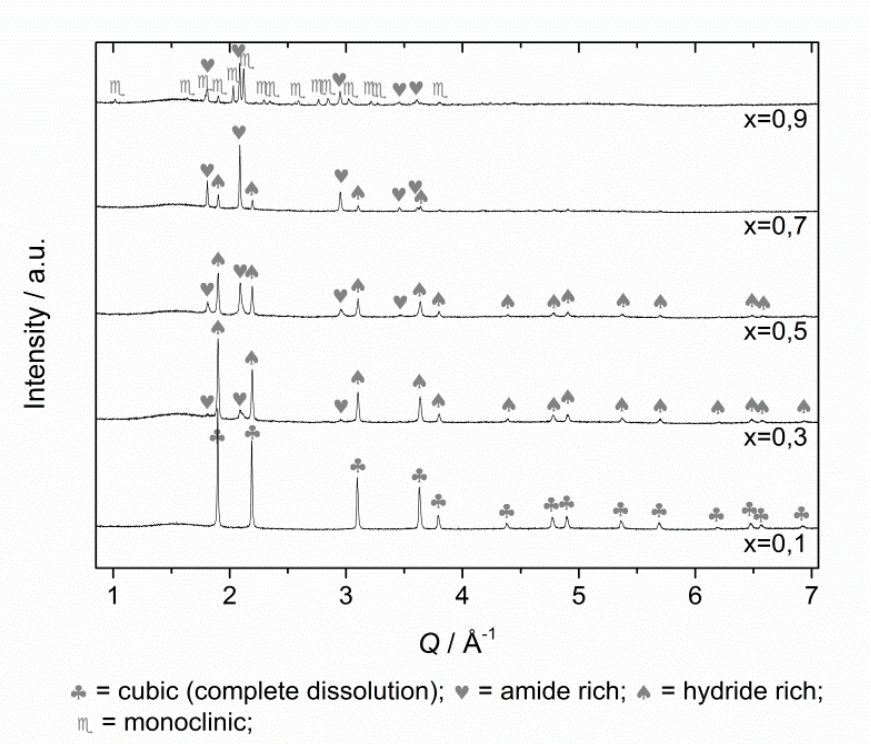

Figure S3. Room temperature diffractograms on the on the x KNH_2 + (1-x) KH samples collected after thermal treatment to 270 °C.

***In situ* synchrotron radiation powder X-ray diffraction (SR-PXD)**

In situ synchrotron X-ray diffraction experiments were performed on five selected compositions (x = 0.1, 0.3, 0.5, 0.7, 0.9), to investigate the behaviour of the K-N-H system upon heat treatment. The pure phases of KH and KNH_2 (indicated as x = 0 and x = 1 respectively) were also measured as reference (Figure S4).

For all the samples with intermediate compositions (x = 0.1, 0.3, 0.5, 0.7, 0.9) the phase transformations of KNH_2 takes place in the expected temperature region. At about 100 °C KNH_2 (F*m*-3*m*) and KH (F*m*-3*m*) are present. At higher temperatures, the change of the diffracted intensities together with the different shift of KNH_2 peaks reveals the starting point of the reaction between the two phases. This reaction continues until ca. 270°C, with a gradual convergence of the two starting structures (an amide-rich- and a hydride-rich phase) to the single phase composition.

In the isothermal part, at 270 °C, the reaction is completed and only one cubic phase is present and appears to be stable for the entire isothermal period, since there are no significant changes of the peaks positions and intensities, independently from the composition. The formation of a single phase for all the compositions is a confirmation of the stability of the solid solution at 270 °C. During the cooling process the only noticeable change is the expected contraction of the cell for the nominal compositions x = 0.1, 0.3, 0.5, 0.7. Only for the composition x = 0.9, a phase transformation to a tetragonal geometry occurs almost at room temperature. Interestingly, since only the tetragonal phase is present, a partial solubility of KH into the tetragonal polymorph of KNH_2 is demonstrated. The structural similarities (highlighted in Figure S1) between the cubic and tetragonal polymorphs are probably responsible for the solubility of small amounts of KH in the tetragonal KNH_2 phase. Moreover, a comparison of this result with the one obtained by *ex situ* PXD on the same composition measured several days after annealing (Figure S3 – x = 0.9) suggests a metastability of the tetragonal phase at room temperature. The solubility of KH in the tetragonal polymorph of KNH_2 could be explained considering the structural similarities between the different polymorphs (Figure S1). Concerning the compositions x = 0.3, 0.5, 0.7, during the cooling process in the *in situ* experiments the kinetic inertia of the system prevents the single phase from disproportioning into two or more cubic phases, as it should be expected according to the *ex situ* data

reported in Figure S3. The Rietveld refinements of the selected pattern at room temperature and at 270 °C are reported in the following figures (Figure S5, S6, S7, S8 and S9).

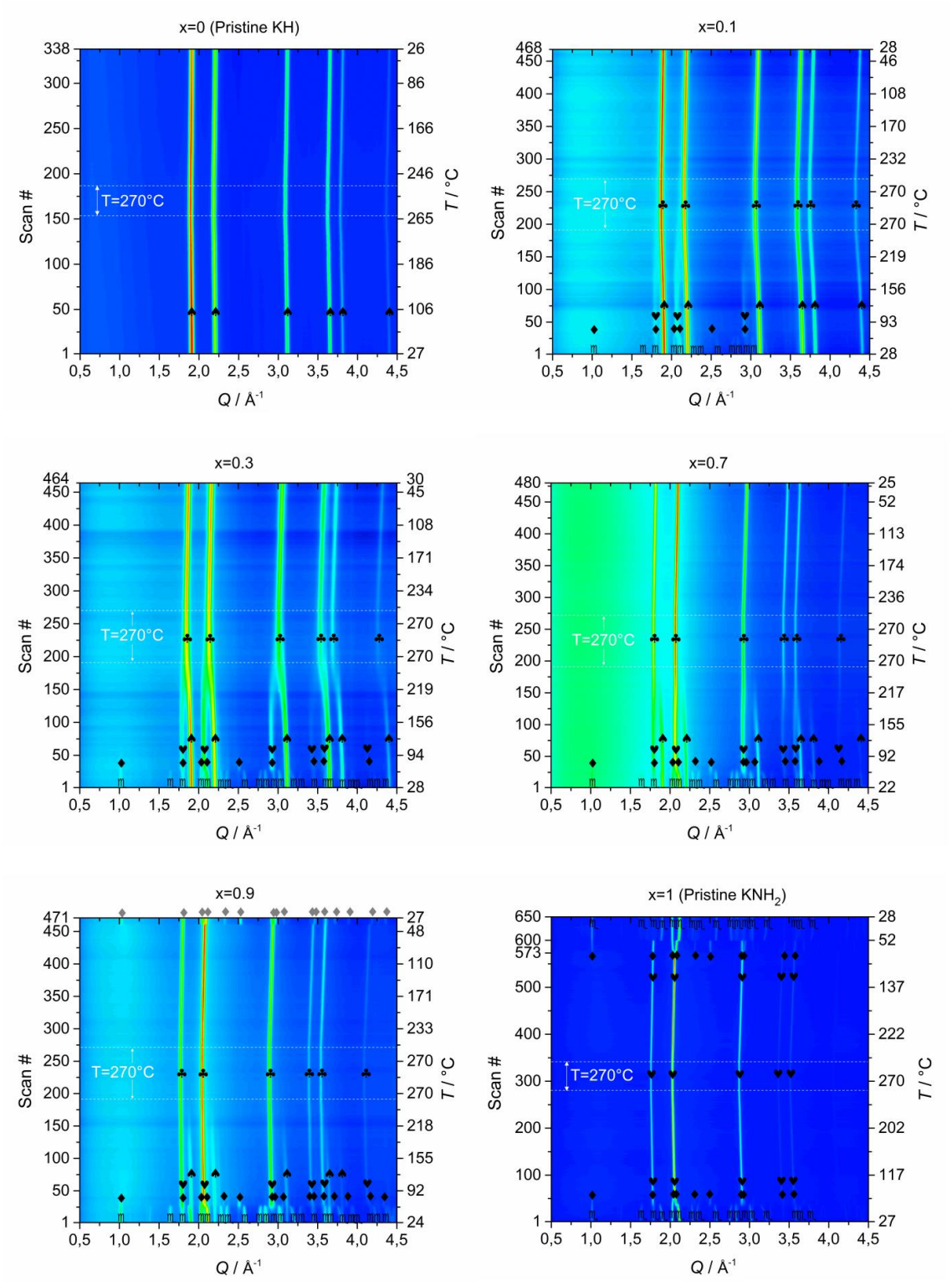

Figure S4. *In situ* SR-PXD measurements of all the compositions x KNH_2 + (1-x) KH (x = 0, 0.1, 0.3, 0.7, 0.9, 1) ℳ = KNH_2 (P121/m1), ♦ = KNH_2 (P4/nmm), ♥ = KNH_2 (Fm-3m), ♣ = $K(NH_2)_xH_{(1-x)}$ (Fm-3m), ⧫ = $K(NH_2)_xH_{(1-x)}$ (P4/nmm).

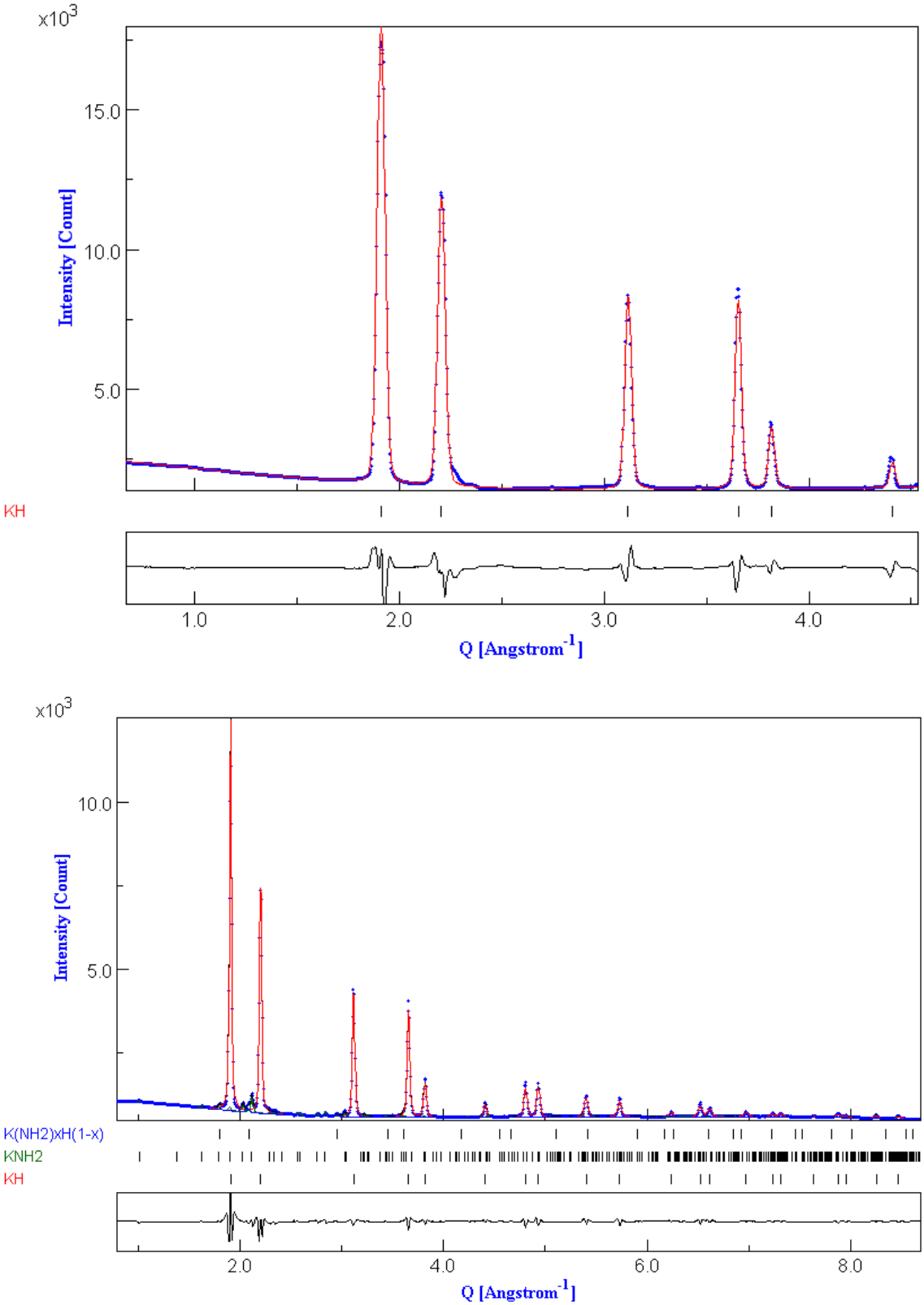

Figure S5. Rietveld refinement of the room temperature SR-PXD pattern of pristine KH (top) and the grinded x KNH_2 + (1 - x) KH sample of nominal composition x = 0.1 (bottom). Rw(%) = 5.01 and Rw(%) = 4.70 respectively.

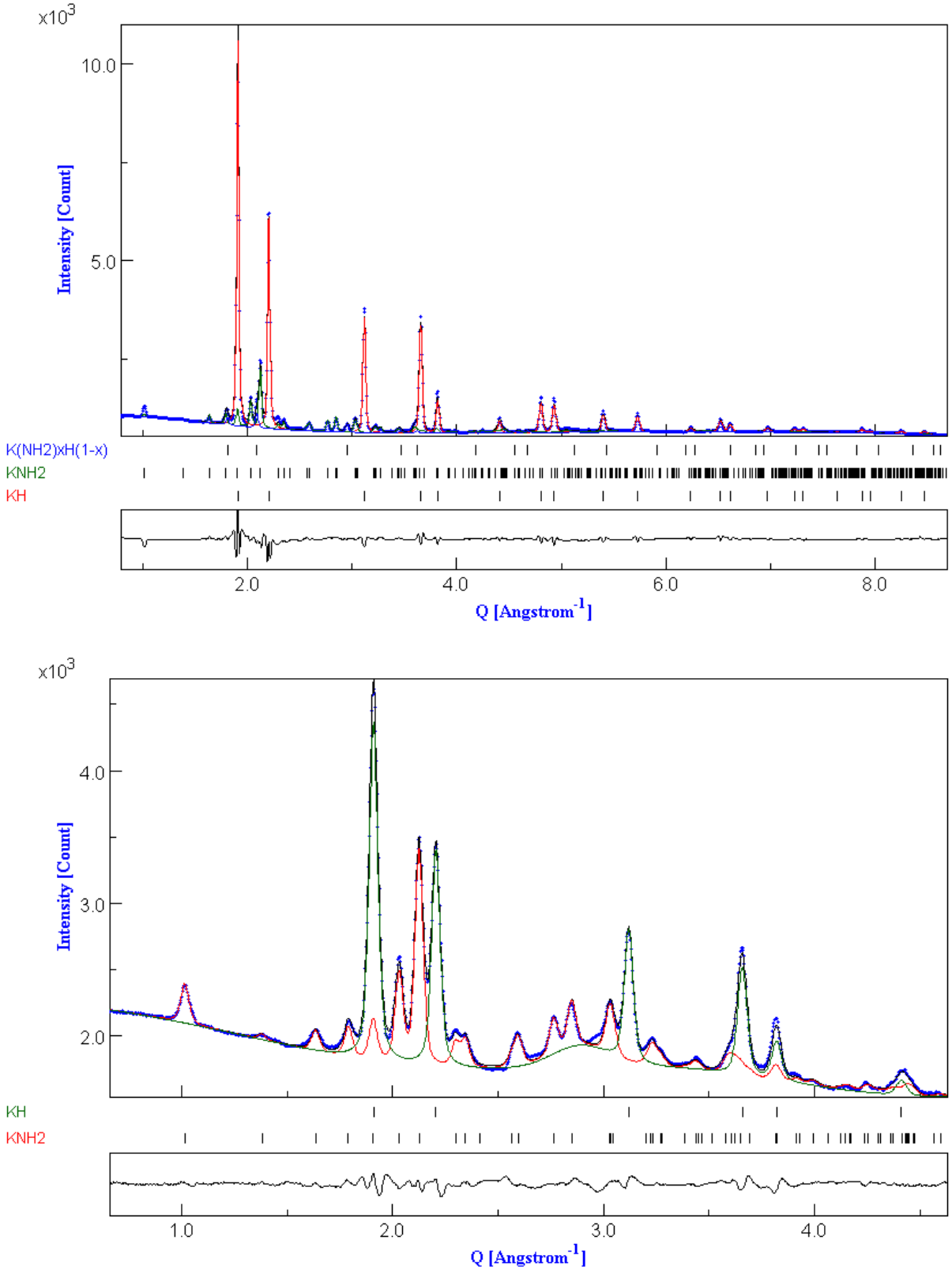

Figure S6. Rietveld refinement of the room temperature SR-PXD pattern of the grinded x KNH_2 + (1 - x) KH samples of nominal composition x = 0.3 (top) and x = 0.5 (bottom). Rw(%) = 4.95 and Rw(%) = 1.05 respectively.

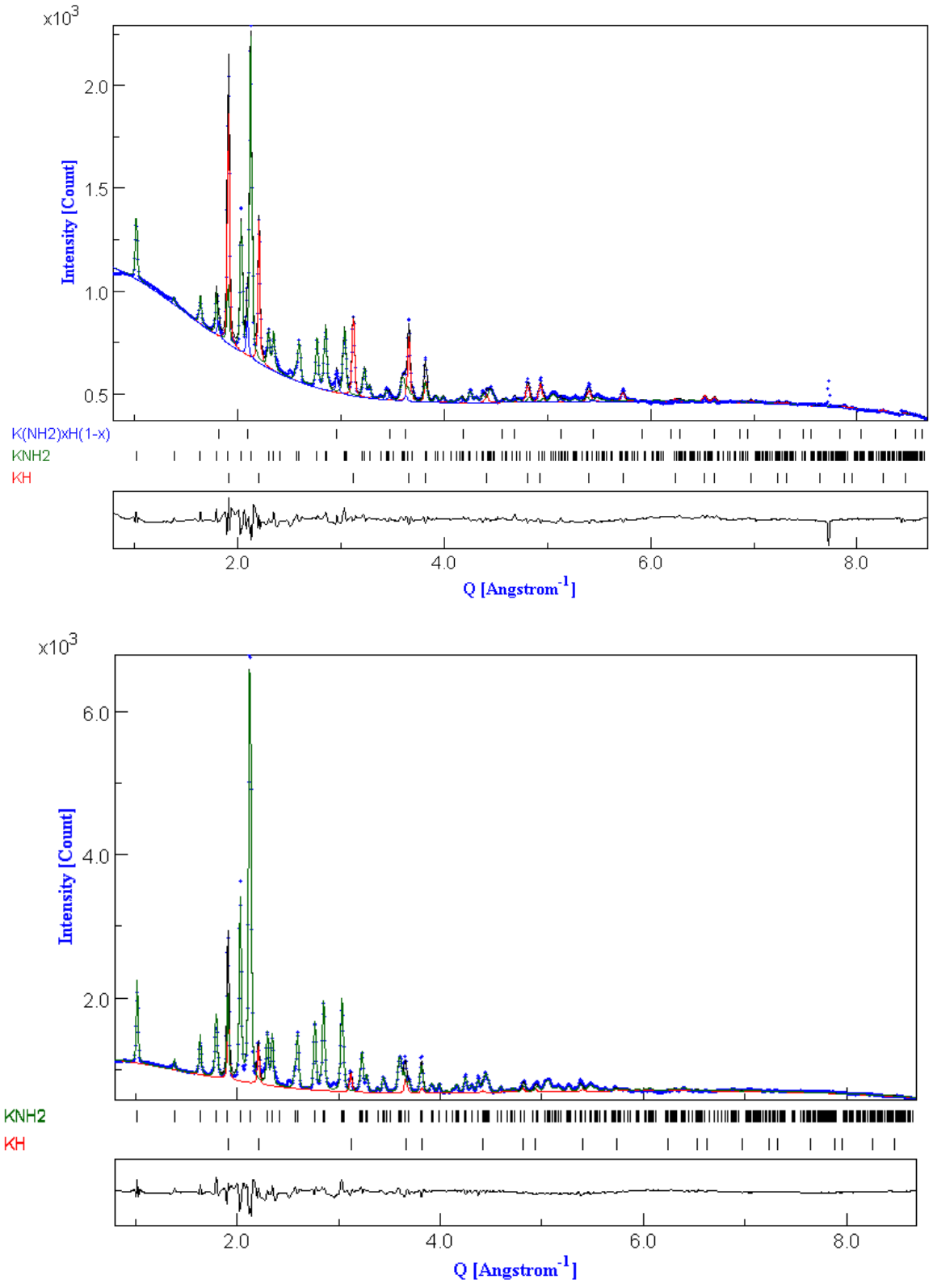

Figure S7. Rietveld refinement of the room temperature SR-PXD pattern of the grinded x KNH_2 + (1 - x) KH samples of nominal composition x = 0.7 (top) and x = 0.9 (bottom). Rw(%) = 2.14 and Rw(%) = 3.37 respectively.

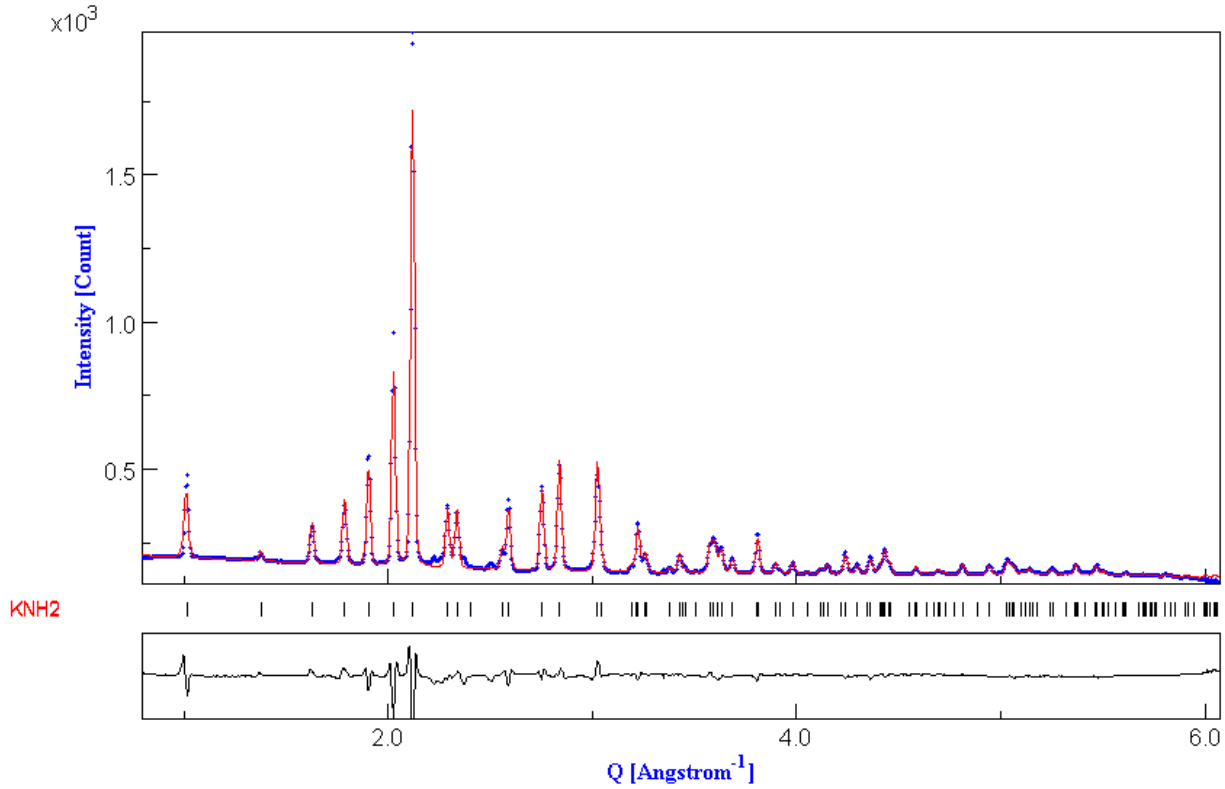

Figure S8. Rietveld refinement of the room temperature SR-PXD pattern of the as obtained KNH_2 sample. Rw(%) = 5.16.

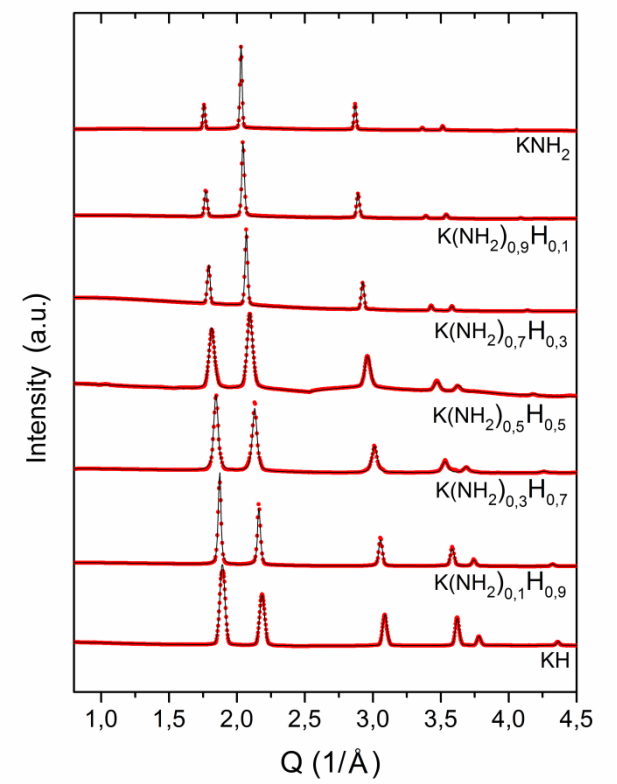

Figure S9. Rietveld refinements of the SR-PXD pattern collected at 270 °C for each composition,

High temperature powder neutron diffraction (PND)

The results obtained by *in situ* SR-PXD are confirmed also by PND on a deuterated sample of nominal composition x = 0.5. The sample was first measured at RT, then transferred in the high temperature cell and measured again in order to be able to remove the contribution of the sample holder by comparison (Figure S10). The sample was then heated up to 270 °C and kept in isotherm during the acquisition of the diffraction pattern.

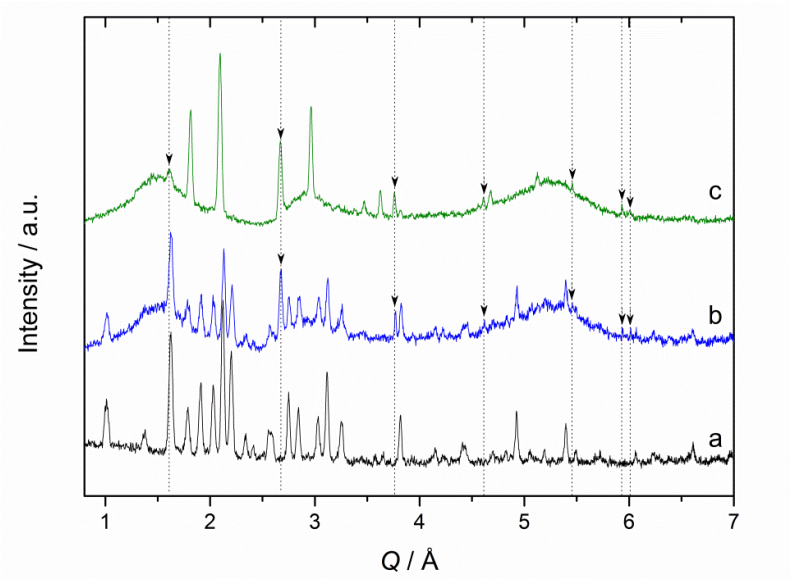

Figure S10. Powder neutron diffraction pattern of the samples 0.5 KND2 + 0.5 KD at RT inside of the vanadium sample holder (a), and the same sample at room temperature (b) and at 270 °C (c) when the quartz sample holder was employed. A wavy background and some new Bragg reflections can be noticed. The peaks generated from the quartz sample holder are indicated by the arrows on the dotted lines and their absence can be noticed in the pattern corresponding to the vanadium sample holder (a).

Figure S11 depicts the Rietveld refinement of the RT diffractogram obtained with the in situ cell.

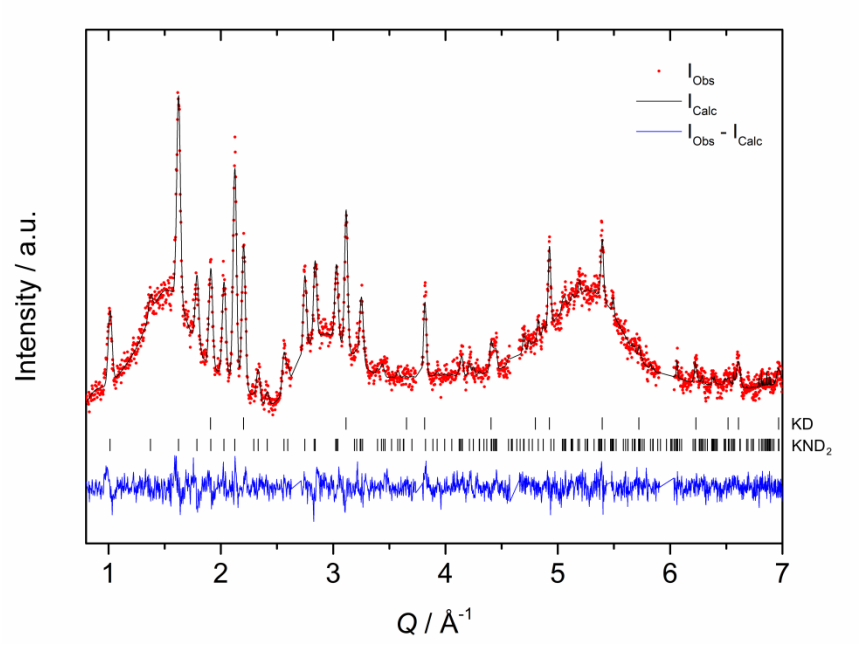

Figure S11. Rietveld refinement of the RT PND pattern of the sample 0.46 KND_2 + 0.54 KD. Rwp(%) = 5.52 (corrected for background).

Nuclear magnetic resonance

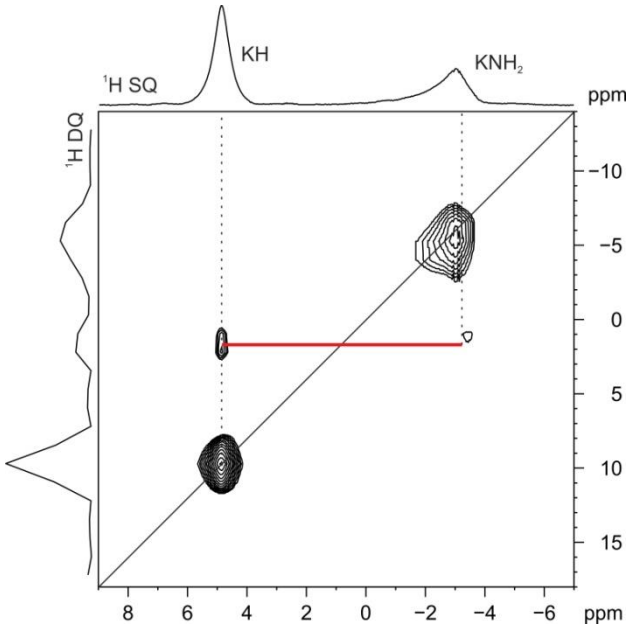

Figure S12. 2D ^{1}H (400.23 MHz) DQ MAS NMR spectrum of the KNH_2 + KH (x = 0.5) after grinding, recorded with a spinning speed of 32 kHz. The red line highlights the DQ correlation between the KH and KNH_2 signal.

Thermal decomposition

The thermal decomposition behavior of the solid solution was determined by differential thermal analysis (DTA) in a Netzsch STA 409 apparatus (Figure S13). After recording the baseline on an empty alumina crucible, about 8 mg of material were heated up in the same crucible under a flow of purified Argon of 50 mL_N/min.

The temperature was increased at 5 °C / min from RT up to 270 °C, kept constant for 10 minutes and then decreased to RT at the

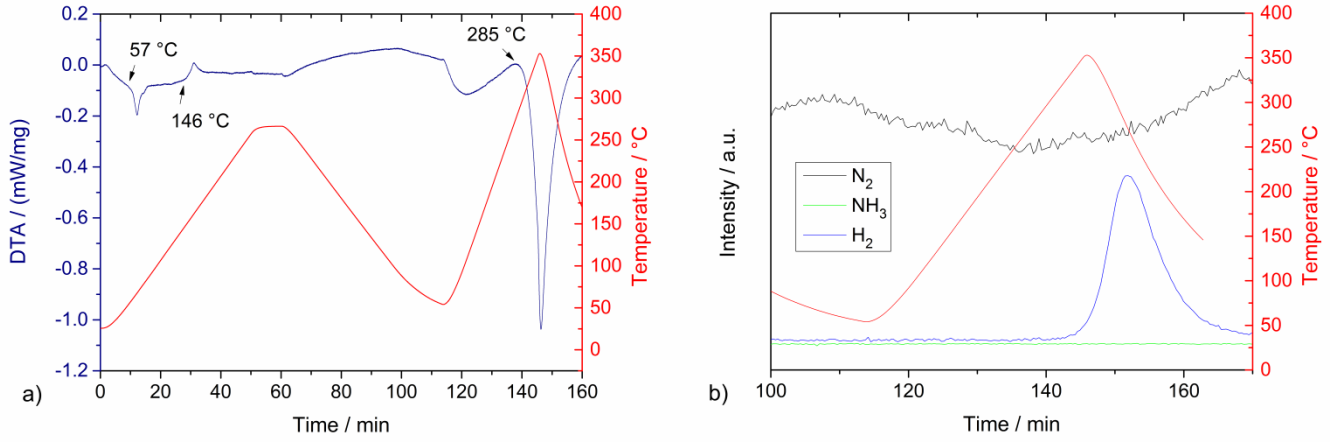

Figure S13. a) DTA measurement performed on the sample x = 0.5 and **b)** mass spectrometer signal during the decomposition process.

same rate in order to observe the formation of the solid solution. During this process an endothermic signal was recorded at ca. 57 °C which is close to the temperature value for the phase transition from the monoclinic to the tetragonal geometry. A less intense peak can be noticed in the shoulder of the main peak, accounting for the phase transition tetragonal → cubic. An exothermic event took place at 146 °C, most probably due to the formation of the solid solution. Right after the cooling process the temperature was increased up to 350 °C with a rate of 10 °C / min to observe the thermal decomposition. A strong endothermic signal can be noticed with an onset temperature of ca. 285 °C, which is ascribable to the starting of the thermal decomposition of the material. According to the mass spectrometer (HidenAnalytical HAL 201) mainly H_2 was released during this event. However the decomposition was not completed even if the temperature rose to 350 °C, therefore the material was heated again, this time up to 400 °C. The decomposition products were detected with the mass spectrometer, revealing formation of H_2, NH_3 and N_2. The interaction of amide/hydride anions is therefore possible at high temperature, however the

inspection of the sample revealed the formation of a shiny metal, suggesting that the powdered sample decomposed completely to form metallic potassium.

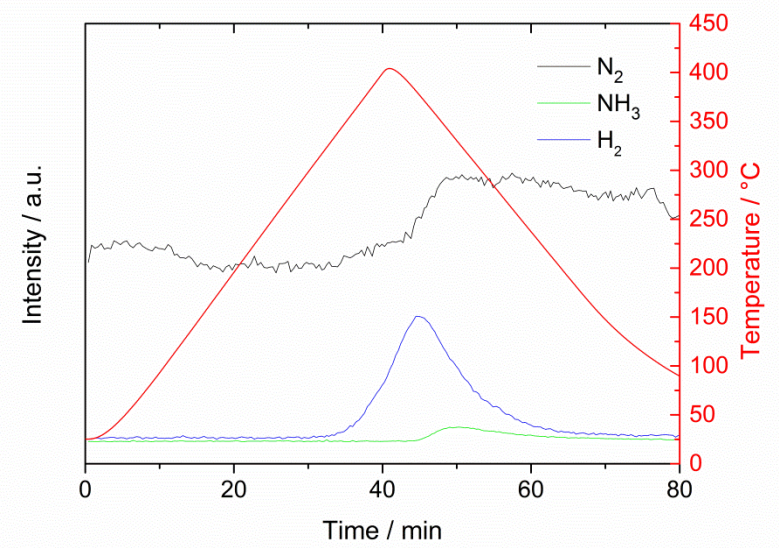

Figure S14. Mass spectrometer signal recorded on the gas flow during the thermal decomposition of the sample x = 0.5.

KNH_2[5] and KH[6] are reported to decompose above 320 °C and above 400°C respectively. However the present results show that, when combined, the two materials start to decompose already at 285 °C, indicating a possible interaction of the two anions to form H_2, while the nitrogen is released from the crystal structure in form of N_2 and NH_3.

References:

1. A. P. Hammersley, S. O. Svensson, M. Hanfland, A. N. Fitch and D. Hausermann, *High Pressure Res*, 1996, **14**, 235-248.
2. L. Lutterotti, S. Matthies, H. R. Wenk, A. S. Schultz and J. W. Richardson, *J Appl Phys*, 1997, **81**, 594-600.
3. V. Favre-Nicolin and R. Cerny, *Journal of Applied Crystallography*, 2002, **35**, 734-743.
4. A. C. L. a. R. B. V. Dreele, *Los Alamos National Laboratory Report LAUR 86-748*, 2000.
5. J. H. Wang, G. T. Wu, Y. S. Chua, J. P. Guo, Z. T. Xiong, Y. Zhang, M. X. Gao, H. G. Pan and P. Chen, *ChemSusChem*, 2011, **4**, 1622-1628.
6. M. Sale, C. Pistidda, A. Taras, E. Napolitano, C. Milanese, F. Karimi, M. Dornheim, S. Garroni, S. Enzo and G. Mulas, *Journal of Alloys and Compounds*, 2013, **580**, S278-S281.